Hindawi Publishing Corporation
Journal of Nanotechnology
Volume 2012, Article ID 323145, 6 pages
doi:10.1155/2012/323145

Research Article

$CoFe_2O_4$–Fe_3O_4 Magnetic Nanocomposites as Photocatalyst for the Degradation of Methyl Orange Dye

Debabrata Mishra,[1] Kula Kamal Senapati,[2] Chandan Borgohain,[2] and A. Perumal[1]

[1] *Department of Physics, Indian Institute of Technology Guwahati, Guwahati 781039, India*
[2] *Central Instrument Facility, Indian Institute of Technology Guwahati, Guwahati 781039, India*

Correspondence should be addressed to A. Perumal, alagarsamy.perumal@gmail.com

Received 23 May 2012; Accepted 10 July 2012

Academic Editor: Mallikarjuna Nadagouda

We report the investigation of temperature-dependent magnetic properties and photocatalytic activity of $CoFe_2O_4$–Fe_3O_4 magnetic nanocomposites (MNCs) synthesized by hydrothermal process. Room-temperature magnetic hysteresis (M-H) loops result enhanced saturation magnetization of 90 emu/g and coercivity (H_C) of 530 Oe for $CoFe_2O_4$–Fe_3O_4 MNCs. With decreasing temperature to 20 K, H_C increases from 500 Oe to 6800 Oe, and the M-H loops exhibit exchange coupling feature between $CoFe_2O_4$ and Fe_3O_4. Low- and high-temperature-dependent magnetization measurements confirm that the blocking temperature lies above 300 K and the presence of two magnetic phase transitions corresponding to $CoFe_2O_4$ and Fe_3O_4, respectively. The photocatalytic activity of the MNCs has been examined on the reduction of methyl orange (MO), a colored compound used in dyeing and printing textiles. The observed results suggest that the $CoFe_2O_4$–Fe_3O_4 MNCs act as an excellent photocatalyst on the degradation of organic contaminants and degrade 93% of MO in 5 hours of UV irradiation. The photocatalytic activity of MNCs is attributed to remarkably high band gap energy and small particle size. Also, the MNCs with a reproducible photocatalytic activity are well separable from water media by applying external magnetic field and acts as a promising catalyst for the remediation of textile wastewater.

1. Introduction

The interest in magnetic nanoparticles (MNPs) and nanocomposites (MNCs) has greatly increased in recent years not only because of their broad applications in several technological fields including ferrofluids, magnetic data storage, magnetooptical, magnetic resonance imaging, medicine, and drug delivery systems, but also due to their relevance from the point of fundamental physics [1–5]. MNPs are also used extensively for catalytic purposes [6]. Photocatalysts utilize photon energy to carry out oxidation and reduction reactions. When irradiated with light energy, an electron (e^-) is excited from the valence band (VB) to the conduction band (CB) of the photocatalyst, leaving a photogenerated hole (h^+). This creates hydroxyl ions in aqueous solution thus facilitating catalytic activities [6, 7]. For a material to qualify as a good photocatalyst needs a relatively large band gap, larger surface area, and nonagglomeration of particles. Agglomeration of particles can be avoided by coating the surface with a surfactant. However, it considerably reduces the magnetic moment of the materials and cannot be reused due to low value of magnetization. That is why development of MNP-based catalyst without surfactant requires greater attention. In particular, tremendous progress has been made in the preparation and processing of MNP-supported catalysts, in view of their high surface area resulting in high catalyst loading capacity [8], high dispersion [9], excellent stability [10], and controllable catalyst recycling without loss in their properties. Magnetic separation renders the recovery of catalyst from liquid-phase reactions much easier and thus dramatically reduces the cost. To fulfill the requirements for various applications, these particles must have suitable magnetic properties (large saturation magnetization (M_S), moderate coercivity (H_C), and high blocking temperature) and also controllable size and shape [11].

Dyes are one of the most notorious contaminants in aquatic environments because of their huge volume

of production from industries, slow biodegradation and decoloration, and toxicity [6]. Methyl orange (MO) is a colored compound used in dyeing and printing textiles, and the release of those colored waste waters in the ecosystem is a source of esthetic pollution in the aquatic life. Therefore, the degradation of MO in cost effective ways without any secondary pollution is very much important for the safety environment [12, 13]. There are several traditional physical techniques such as adsorption, ultrafiltration, reverse osmosis, coagulation, chlorination, ozonation, and biodegradation for the removal of dye pollutants [14, 15]. Nevertheless, most of the above techniques transfer organic compound from water to another phase, thus causing secondary pollution. On the other hand, photocatalytic processes are environmentally friendly methods that utilize radiation energy to perform catalysis under ambient conditions and thus appear as the most emerging technology [16, 17]. However, the application of photocatalytic procedures using MNPs/MNCs for remediation of textile waste water is rather limited to only a few investigations.

Among other MNP materials, fine Cobalt ferrite particles have been used as MNP-based catalysts due to their strong interparticle interactions and nonagglomeration behaviors [19]. Also, it has strong anisotropy, high H_C, and moderate M_S along with the good mechanical hardness and chemical stability. The catalytic activities of MNPs can further be enhanced by preparing a suitable hybrid nanocomposite with other MNPs. This facilitates a new composite material with novel magnetic, electrical, and optical properties. Various preparation methods such as sonochemical reactions, mechanochemical synthesis, hydrolysis, hydrothermal, and aqueous coprecipitation have generally been used to make nanocomposites with desired properties [18, 20, 21]. In this study, we have employed hydrothermal process to prepare $CoFe_2O_4$–Fe_3O_4 nanocomposites and investigated their temperature-dependent magnetic properties. Also, the photocatalytic activity of the MNC on the degradation of environmental pollutants (MO) was explored for the first time.

2. Experimental Details

Magnetic nanocomposites of $CoFe_2O_4$–Fe_3O_4 were prepared by hydrothermal method. All the reactants and the reagents used for the preparation of MNCs were high-purity commercially available $CoCl_2 \cdot 6H_2O$ (99%), $FeCl_3 \cdot 6H_2O$ (99%), NaOH (96%), and PEG-400 (99%) and used as received. In a typical procedure, $CoCl_2 \cdot 6H_2O$ (1 g in 50 mL PEG-400, 4.2 mmol) and $FeCl_3$ (1.6 g in 50 mL PEG-400, 10.3 mmol) solutions were mixed and stirred in a magnetic stirrer. Subsequently, NaOH (3 M, 25 mL distilled deionized water) solution was added dropwise and stirred for half an hour at 80°C. Then, the solution (dark brown) was transferred into an autoclave and heated at 200°C for 12 hours. After this, the resulting black precipitate was first washed with alcohols to remove the PEG and with water for the complete removal of NaOH content. Eventually, the product was washed with dried ethanol and dried at 200°C under vacuum. Crystal structure of the as-prepared and annealed samples were examined by X-ray diffraction (XRD) using a Rigaku TTRAX diffractometer with Cu-K_α radiation and transmission electron microscopy (TEM) using a JEOL 2100 microscopy. Room temperature and temperature-dependent magnetic properties were measured by vibrating sample magnetometer (VSM, Lake Shore Model 7410). Optical properties were measured by PerkinElmer RXI FT-IR spectrometer in KBr pellet and Varian Cary 50 UV spectrophotometer. The BET surface area of the MNCs was analyzed by the Chemisorb surface area analyzer (Make: Micromeritics, Model: Chemisorb 2720) with pretreatment of 0.03 g of the sample by degassing at 200°C for 3 minutes under helium gas.

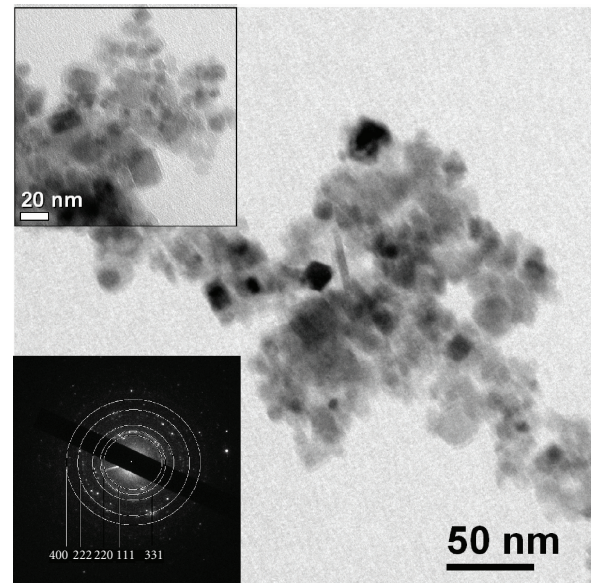

Figure 1: BF TEM micrographs and SAED patterns of as-prepared $CoFe_2O_4$–Fe_3O_4 magnetic nanocomposites.

3. Results and Discussion

Figure 1 shows bright-field (BF) TEM micrographs and selected area electron diffraction (SAED) pattern of as-prepared $CoFe_2O_4$–Fe_3O_4 MNC. The micrographs show the fine nonagglomerated particles with the average particle size of about 20 nm, which are highly desirable for the catalytic activity. SAED pattern shows that MNCs are crystalline in nature, and the peak profile represents the cubic spinel structure of $CoFe_2O_4$ and Fe_3O_4, which is consistent with the XRD analysis (not shown here). To confirm the spinel structure of the MNCs, infrared (IR) absorption spectra were obtained in the range between 350 cm^{-1} are 1000 cm^{-1}, and the same are depicted in Figure 2(a). It is found that the spectra consist of two significant absorption bands, first at about 590 cm^{-1} (ν_1) and second at about 410 cm^{-1} (ν_2). Absorption bands observed in this range reveal the formation of single phase spinel structure having two sublattices, which are assigned to tetrahedral site (ν_1) and octahedral site (ν_2) [22]. In addition,

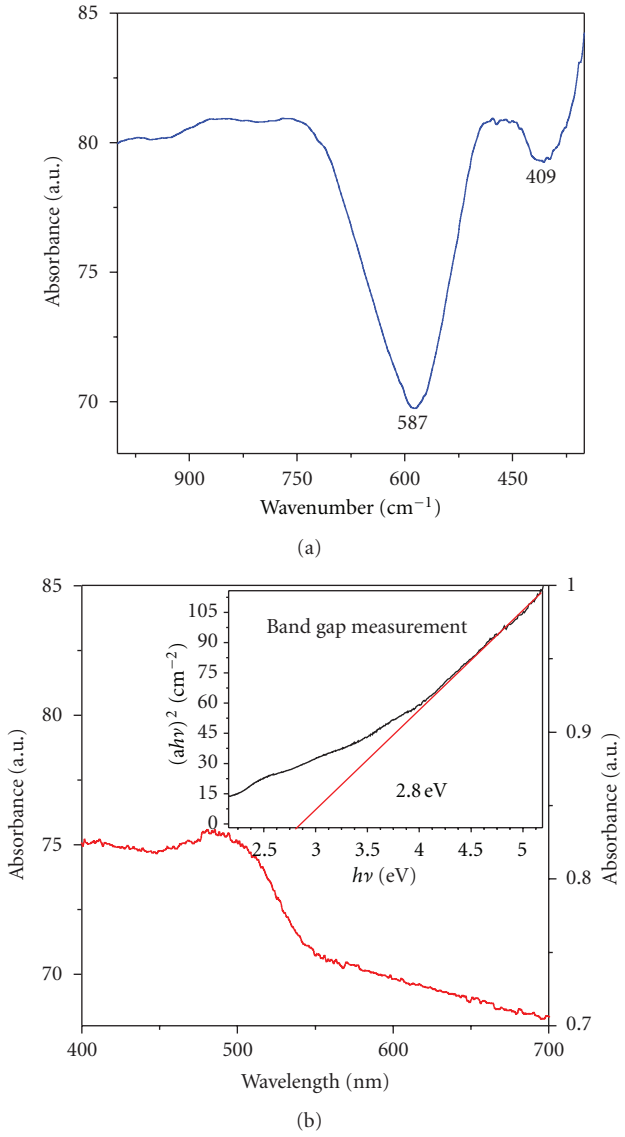

FIGURE 2: (a) IR and (b) UV-vis spectra of as-prepared $CoFe_2O_4$–Fe_3O_4 magnetic nanocomposites. Inset: Plot of $(\alpha h\nu)^2$ versus $h\nu$ to determine the band gap energy using Tauc relation [18].

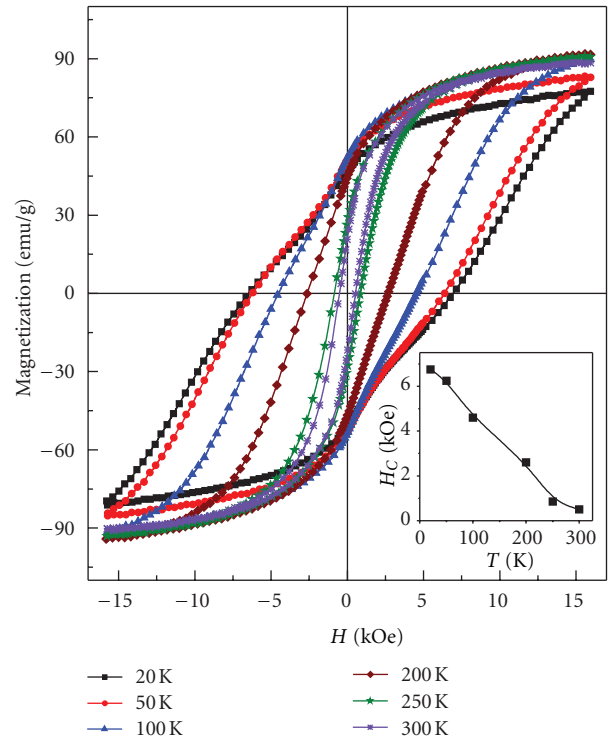

FIGURE 3: Magnetic hysteresis of as-prepared $CoFe_2O_4$–Fe_2O_3 magnetic nanocomposites obtained at different temperature between 20 K and 300 K. Inset: Variation of coercivity with temperature.

the formation of soft Fe_3O_4 phase in the nanocomposite has been confirmed by the UV analysis as shown in Figure 2(b). In case of magnetic nanoparticles, the UV absorption band is observed in the region 330–500 nm, which originates primarily from the absorption and scattering of light by the magnetic nanoparticles. The band gap energy was determined from the absorption spectra using Tauc relation [23], as shown in the inset of Figure 2(b), and found to be around 2.8 eV. It should be mentioned here that with higher band gap energy, the recombination rate of electrons and hole pairs are retarded, and photocatalytic properties are enhanced.

To understand the magnetic properties of $CoFe_2O_4$–Fe_3O_4 MNCs, temperature, dependent magnetic hysteresis (M-H) loops were measured in the temperature range from 20 K to 300 K, and the same are displayed in Figure 3. It can be seen that the MNCs exhibit a clear hysteresis at 300 K but do not saturate at 15 kOe applied field due to the strong anisotropy. H_C is about 500 Oe at 300 K. This suggests that the MNCs are not in superparamagnetic state in room temperature, in contrast to the earlier observation in $CoFe_2O_4$ nanoparticles [20, 24]. Also, the magnetization value obtained at 15 kOe-applied field (M_S) is about 90 emu/g, which is higher than the value (~65 emu/g) reported for $CoFe_2O_4$ particles with the similar particle size [25]. This confirms that the intrinsic properties of MNPs can be modified (enhanced) by making MNCs with the properly chosen materials. In the present investigation, the nanocomposite of $CoFe_2O_4$ with Fe_3O_4 was prepared, and the enhancement in M_S can be attributed to large magnetocrystalline anisotropy and higher interparticle interactions in $CoFe_2O_4$–Fe_3O_4 MNCs [19]. It is to be noted that for catalytic applications MNPs should have better magnetic properties for convenient catalyst recycling. On the other hand, with decreasing temperature up to 200 K, the MNCs exhibit almost similar loops, but H_C increases from 500 Oe at 300 K to 2650 Oe at 200 K. On further lowering the temperature, not only the H_C increases to 6600 at 20 K, but also the loops exhibit a kink around the remanence during the magnetization reversal process. This suggests the presence of magnetic exchange coupling between the hard magnetic $CoFe_2O_4$ and soft magnetic Fe_3O_4 MNPs and interparticle interactions in the presently

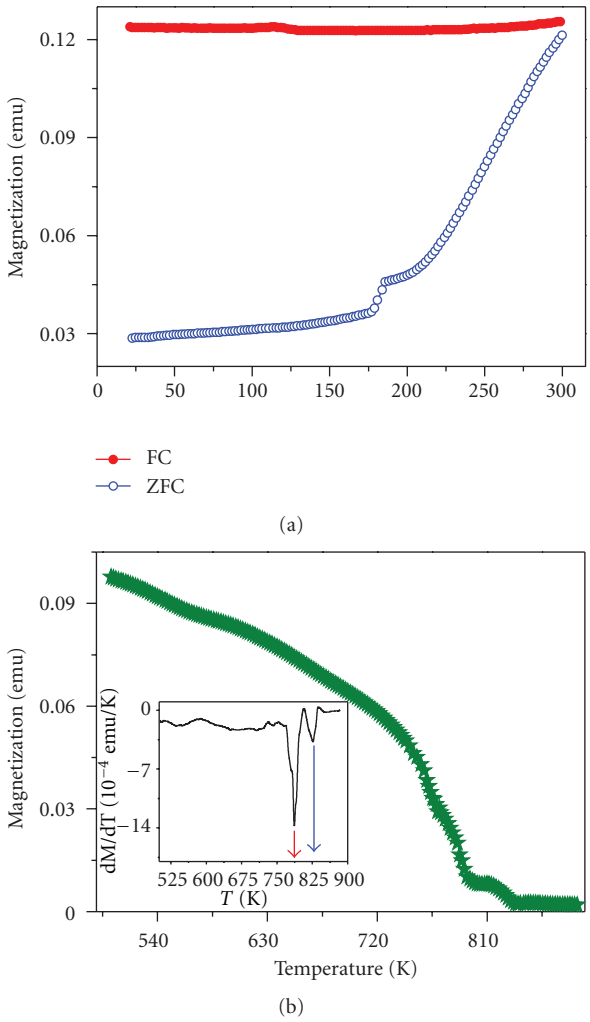

Figure 4: Temperature dependent magnetization curves measured at an applied field of 200 Oe (a) at low temperatures between 20 and 300 K under ZFC and FC conditions and (b) at high temperatures for as-prepared $CoFe_2O_4$–Fe_2O_3 magnetic nanoparticles. Inset: Plot of thermal derivative of magnetization with temperature.

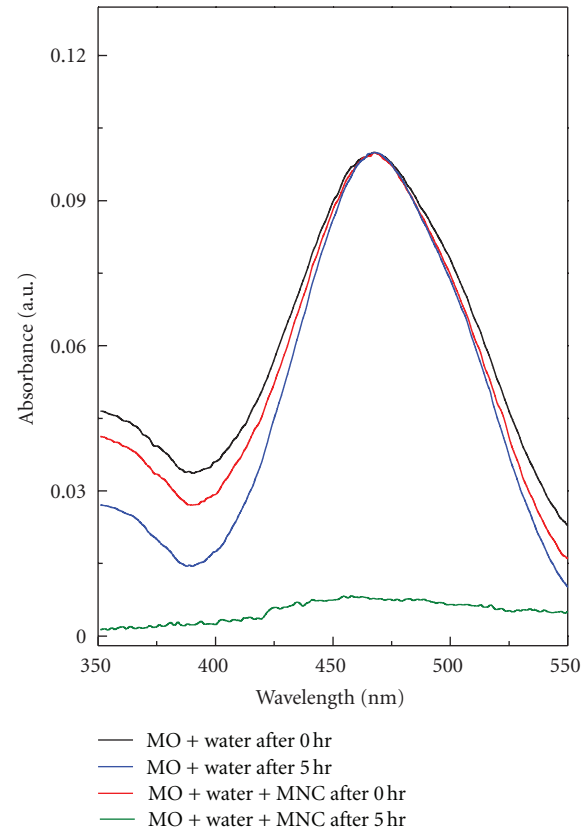

Figure 5: Absorbance spectra of methyl orange loaded with and without MNCs/water and UV irradiation for 5 hours. The irradiation was carried out with a 12 mW Xenon lamp with a main wavelength of 400 nm.

investigated samples [24]. Such a ferromagnetic exchange coupling is desirable for higher magnetization value of composites. Temperature-dependent magnetization measurement measured at a magnetic field of 100 Oe under zero-field-cooled (ZFC) and field-cooled (FC) conditions as shown in Figure 4(a) confirms that the blocking temperature lies about room temperature. On the other hand, high-temperature magnetization data (Figure 4(b)) depicts the presence of two clear phase transitions corresponding to $CoFe_2O_4$ and Fe_3O_4 at 790 K [26] and 840 K [27], respectively.

Photocatalytic activity of prepared MNCs was evaluated by photocatalytic decomposition of MO in aqueous solution at ambient temperature. $CoFe_2O_4$–Fe_3O_4 MNC (0.02 g) was placed into the tubular quartz vessel containing 100 mL of 1×10^{-5} M MO aqueous solutions and mixed by ultrasonication for 10 min. Subsequently, the mixture was stirred in dark to obtain adsorption/desorption equilibrium until the concentration of MO was constant and then illuminated with a UV lamp. The absorption spectra, obtained using UV-vis spectrophotometer, are illustrated in Figure 5. It can be seen that a maximum absorbance was observed around 465 nm for two cases: (i) for the mixture of MO and water in as-mixed state and (ii) for the mixture of MO and water exposed to UV light for five hours. Also, the as-mixed mixture of MO, water, and MNCs without irradiation showed a maximum absorbance around 465 nm. These results suggest that no MO degradation occurs in these mixtures. However, a typical run performed for the mixture containing MO, water, and the MNCs without UV radiation in dark for 5 hours has revealed a minor change in the maximum absorption around 465 nm (less than 5%), as compared to the initial absorbance of the as-mixed mixture of MO, water, and the MNCs. This is mainly due to the sorption of dye molecules by the MNCs. On the other hand, the maximum absorbance almost disappears for the mixture containing MO, water, and MNCs subjected to UV irradiation for 5 hours. These results confirm that the effective degradation of the dye occurs only in the presence of UV irradiation, and this is the first time we are reporting $CoFe_2O_4$–Fe_3O_4 MNC as a new photocatalyst to degrade

MO organic contaminant. The photocatalytic degradation percentage of MO was calculated using

$$\text{Degradation } (\%) = \left(\frac{A_0 - A}{A_0}\right) \times 100, \quad (1)$$

where A_0 is the initial absorbance of MO before degradation, and A is the absorbance after time t. The degradation percentage of MO by MNC is 93% in 5 h of UV irradiation at a pH range of 5 to 6. This can be attributed to (a) high band gap energy (2.8 eV) for the MNCs as the photocatalytic effect depends on the enhancement in electron-hole separation [28], and (b) small particle size which is associated with high surface area. The BET surface area of the $CoFe_2O_4$–Fe_3O_4 MNCs analyzed using chemisorb surface area analyzer was found to be 112 m^2/g with a total pore volume of 0.0565 m^2/g. This is significantly larger for this type of magnetic materials, and hence it accounts for one of the reasons for the presently observed high photocatalytic activities. Also, the pH value of the dye solution plays a major role in the photodegradation of the dye, as the adsorption of the dye molecules on the catalyst surface is pH dependent [29, 30]. For the presently studied system, we have obtained the optimum degradation of the dye in the low acidic pH (pH ~5-6).The degradation of MO using TiO_2-, and ZnS-based semiconductors has also been reported [31, 32]. However, the shape of the nanoparticles poses a limit in the photocatalytic activity, and an efficient technique is needed for the facile separation of the catalyst. On the other hand, the MNCs can be synthesized easily with the better control of size and shape, and well separated from the media by applying the external magnetic field.

4. Conclusion

$CoFe_2O_4$–Fe_3O_4 magnetic nanocomposites with the average particle size of 20 nm were synthesized by hydrothermal process, and the formation of nanocomposites was confirmed through TEM, XRD, IR, and UV-vis spectroscopy studies. Enhanced magnetization of 90 emu/g and a coercivity of 500 Oe were obtained at room temperature. The blocking temperature of the nanocomposites was found to be above room temperature. Low- and high-temperature magnetization measurements confirmed the existence of magnetic exchange coupling between $CoFe_2O_4$ and Fe_3O_4 and their phase transitions, respectively. Photocatalytic activity of the MNCs was confirmed on methyl orange under UV irradiation and found to be effective on degrading the methyl orange at ambient temperature. MNCs could also be well separated magnetically without losing its photocatalytic activity.

Acknowledgments

This work was financially supported by DAE-BRNS, India, vide project no. 2005/20/34/1/BRNS/376. Infrastructural facilities (XRD, VSM, and TEM), provided by DST vide project nos SR/FST/PII-020/209, SR/S2/CMP-19/2006, and SR/S5/NM-108/2006, are gratefully acknowledged.

References

[1] M. V. Berkovsky, F. V. Medvedev, and S. M. Krakov, *Magnetic Fluids: Engineering Applications*, Oxford University Press, Oxford, UK, 1993.

[2] M. H. Kryder, "Ultrahigh-density recording technologies," *MRS Bulletin*, vol. 21, no. 9, pp. 17–19, 1996.

[3] A. P. Alivisatos, "Semiconductor clusters, nanocrystals, and quantum dots," *Science*, vol. 271, no. 5251, pp. 933–937, 1996.

[4] K. V. P. M. Shafi, A. Gedanken, R. Prozorov, and J. Balogh, "Sonochemical preparation and size-dependent properties of nanostructured $CoFe_2O_4$ particles," *Chemistry of Materials*, vol. 10, no. 11, pp. 3445–3450, 1998.

[5] Y. Zhu, L. P. Stubbs, F. Ho et al., "Magnetic nanocomposites: a new perspective in catalysis," *ChemCatChem*, vol. 2, no. 4, pp. 365–374, 2010.

[6] E. Casbeer, V. K. Sharma, and X.-Z. Li, "Synthesis and photocatalytic activity of ferrites under visible light: a review," *Separation and Purification Technology*, vol. 87, pp. 1–14, 2012.

[7] H. Zhang, G. Chen, and D. W. Bahnemann, "Photoelectrocatalytic materials for environmental applications," *Journal of Materials Chemistry*, vol. 19, no. 29, pp. 5089–5121, 2009.

[8] P. D. Stevens, J. Fan, H. M. R. Gardimalla, M. Yen, and Y. Gao, "Superparamagnetic nanoparticle-supported catalysis of Suzuki cross-coupling reactions," *Organic Letters*, vol. 7, no. 11, pp. 2085–2088, 2005.

[9] A.-H. Lu, E. L. Salabas, and F. Schüth, "Magnetic nanoparticles: synthesis, protection, functionalization, and application," *Angewandte Chemie*, vol. 46, pp. 1222–1244, 2007.

[10] M. A. G. Soler, E. C. D. Lima, S. W. Da Silva et al., "Aging investigation of cobalt ferrite nanoparticles in low pH magnetic fluid," *Langmuir*, vol. 23, no. 19, pp. 9611–9617, 2007.

[11] V. F. Puntes, K. M. Krishnan, and A. P. Alivisatos, "Colloidal nanocrystal shape and size control: the case of cobalt," *Science*, vol. 291, no. 5511, pp. 2115–2117, 2001.

[12] H. Kyung, J. Lee, and W. Choi, "Simultaneous and synergistic conversion of dyes and heavy metal ions in aqueous TiO_2 suspensions under visible-light illumination," *Environmental Science and Technology*, vol. 39, no. 7, pp. 2376–2382, 2005.

[13] H. Zollinger, *Color Chemistry: Synthesis, Properties and Applications of Organic Dyes and Pigments*, VCH Publishers, New York, NY, USA, 1987.

[14] H. Lachheb, E. Puzenat, A. Houas et al., "Photocatalytic degradation of various types of dyes (Alizarin S, Crocein Orange G, Methyl Red, Congo Red, Methylene Blue) in water by UV-irradiated titania," *Applied Catalysis B*, vol. 39, no. 1, pp. 75–90, 2002.

[15] W. S. Kuo and P. H. Ho, "Solar photocatalytic decolorization of methylene blue in water," *Chemosphere*, vol. 45, no. 1, pp. 77–83, 2001.

[16] S. Vaidyanathan, K. R. Ryan, and E. W. Eduardo, "Synthesis and UV-visible-light photoactivity of noble-metal-$SrTiO_3$ composites," *Industrial and Engineering Chemistry Research*, vol. 45, no. 7, pp. 2187–2193, 2006.

[17] D. L. Liao and B. Q. Liao, "Shape, size and photocatalytic activity control of TiO_2 nanoparticles with surfactants," *Journal of Photochemistry and Photobiology A*, vol. 187, no. 2-3, pp. 363–369, 2007.

[18] S. Bhattacharyya, J. P. Salvetat, R. Fleurier, A. Husmann, T. Cacciaguerra, and M. L. Saboungi, "One step synthesis of highly crystalline and high coercive cobalt-ferrite nanocrystals," *Chemical Communications*, no. 38, pp. 4818–4820, 2005.

[19] C. R. Vestal, Q. Song, and Z. J. Zhang, "Effects of interparticle interactions upon the magnetic properties of $CoFe_2O_4$ and $MnFe_2O_4$ nanocrystals," *Journal of Physical Chemistry B*, vol. 108, no. 47, pp. 18222–18227, 2004.

[20] F. Bensebaa, F. Zavaliche, P. L'Ecuyer, R. W. Cochrane, and T. Veres, "Microwave synthesis and characterization of Co-ferrite nanoparticles," *Journal of Colloid and Interface Science*, vol. 277, no. 1, pp. 104–110, 2004.

[21] R. T. Olsson, G. Salazar-Alvarez, M. S. Hedenqvist, U. W. Gedde, F. Lindberg, and S. J. Savage, "Controlled synthesis of near-stoichiometric cobalt ferrite nanoparticles," *Chemistry of Materials*, vol. 17, no. 20, pp. 5109–5118, 2005.

[22] R. D. Waldron, "Infrared spectra of ferrites," *Physical Review*, vol. 99, no. 6, pp. 1727–1735, 1955.

[23] J. Tauc, *Amorphous and Liquid Semiconductor*, Plenum, New York, NY, USA, 1974.

[24] S. Ammar, A. Helfen, N. Jouini et al., "Magnetic properties of ultrafine cobalt ferrite particles synthesized by hydrolysis in a polyol medium," *Journal of Materials Chemistry*, vol. 11, no. 1, pp. 186–192, 2001.

[25] Z. Gu, X. Xiang, G. Fan, and F. Li, "Facile synthesis and characterization of cobalt ferrite nanocrystals via a simple reduction-oxidation route," *Journal of Physical Chemistry C*, vol. 112, no. 47, pp. 18459–18466, 2008.

[26] S. T. Alone and K. M. Jadhav, "Structural and magnetic properties of zinc- and aluminum-substituted cobalt ferrite prepared by co-precipitation method," *Pramana*, vol. 70, no. 1, pp. 173–181, 2008.

[27] A. Chakraborty, "Kinetics of the reduction of hematite to magnetite near its Curie transition," *Journal of Magnetism and Magnetic Materials*, vol. 204, no. 1, pp. 57–60, 1999.

[28] J. Yu, J. Xiong, B. Cheng, and S. Liu, "Fabrication and characterization of Ag-TiO_2 multiphase nanocomposite thin films with enhanced photocatalytic activity," *Applied Catalysis B*, vol. 60, no. 3-4, pp. 211–221, 2005.

[29] I. K. Konstantinou and T. A. Albanis, "TiO_2-assisted photocatalytic degradation of azo dyes in aqueous solution: kinetic and mechanistic investigations: a review," *Applied Catalysis B*, vol. 49, no. 1, pp. 1–14, 2004.

[30] H. Lachheb, E. Puzenat, A. Houas et al., "Photocatalytic degradation of various types of dyes (Alizarin S, Crocein Orange G, Methyl Red, Congo Red, Methylene Blue) in water by UV-irradiated titania," *Applied Catalysis B*, vol. 39, no. 1, pp. 75–90, 2002.

[31] T. Puangpetch, T. Sreethawong, S. Yoshikawa, and S. Chavade, "Synthesis and photocatalytic activity in methyl orange degradation of mesoporous-assembled $SrTiO_3$ nanocrystals prepared by sol–gel method with the aid of structure-directing surfactant," *Journal of Molecular Catalysis A*, vol. 287, p. 70, 2008.

[32] C. Wang, X. Wang, B.-Q. Xu et al., "Enhanced photocatalytic performance of nanosized coupled ZnO/SnO_2 photocatalysts for methyl orange degradation," *Journal of Photochemistry and Photobiology A*, vol. 168, pp. 47–52, 2004.